

Brain mapping tools for neuroscience research

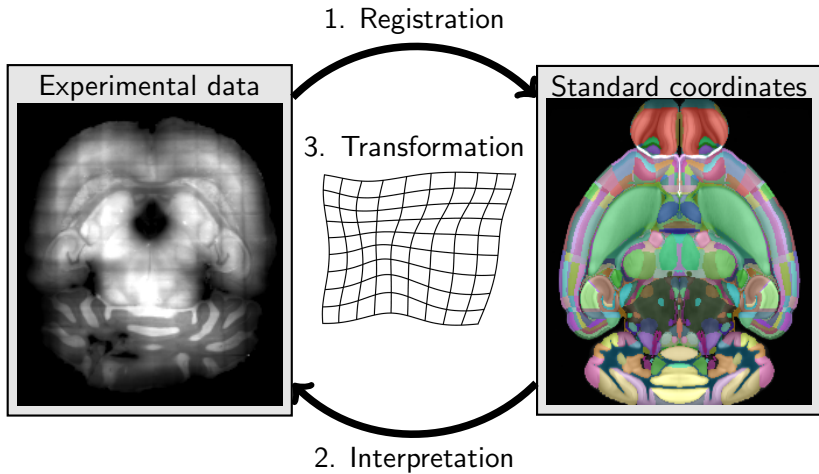
Devin Crowley (devin.g.crowley@gmail.com)

NeuroData and Center for Imaging Science
Department of Biomedical Engineering
Johns Hopkins University

Workshop Outline

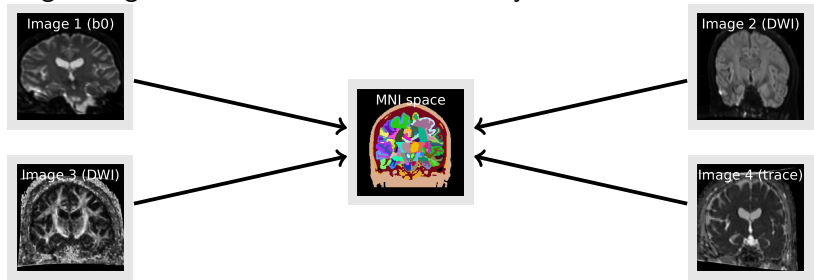
1. Focused look at registration algorithms
2. Running code on real data
3. Discussion of issues affecting the community

The goal of brain mapping



1. Registration

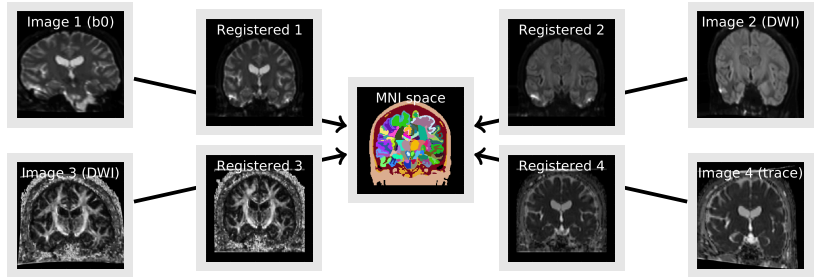
Align images into a standard coordinate system



- ▶ Enrich information by fusing modalities
- ▶ Analyze different specimens statistically
- ▶ Build databases of information indexed to spatial coordinates

1. Registration

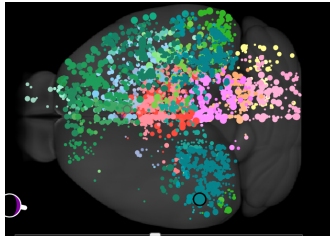
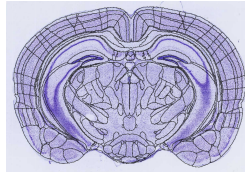
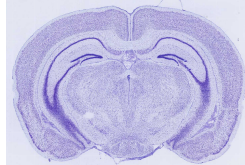
Align images into a standard coordinate system



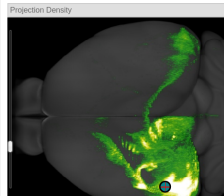
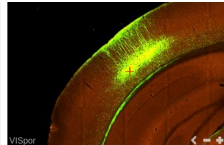
- ▶ Enrich information by fusing modalities
- ▶ Analyze different specimens statistically
- ▶ Build databases of information indexed to spatial coordinates

2. Interpretation

Leverage information stored in atlas coordinates.¹
MBA ARA



Injection Structure(s)	Mouse Line	Tracer	Inj Site Vol
VISpor - VISal, VISl, Visp, Vispl, VISl, TEa	Rbp4-Cre_KL100	SypEGFP	0.400
VISpor - TEa, ECT, ENTl, ENTm, SUB	Cux2-IRES-Cre	EGFP	0.355
VISpor - VISl, Vispl	Tlx3-Cre_Pl56	EGFP	0.012
VISpor - VISl, ENTl, ENTm, SUB	Syt6-Cre_K114B	EGFP	0.007
VISpor - VISl, VISl, TEa, ECT, ENTl, ENTm, SUB	A930038C07R1... ACAd - ACAd	EGFP	0.103
ACAd - ACAd	Chrm2-Cre_O...	EGFP	0.052

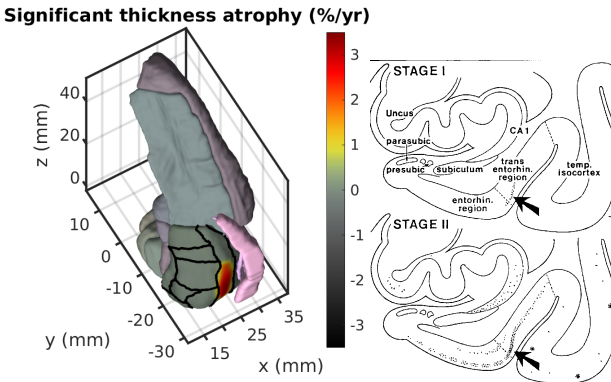


- ▶ Label images with standard ontologies
- ▶ Index to gene expression, cell types, tractography, etc.

¹MBA: Mouse brain architecture brainarchitecture.org, ARA: Allen reference atlas connectivity.brain-map.org/

3. Transformation

Studying transformations quantifies growth or atrophy

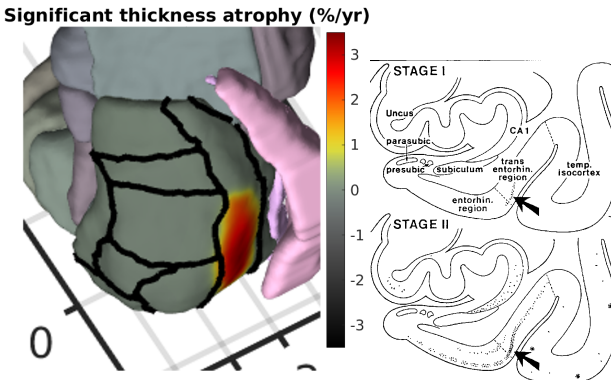


- ▶ Here thickness change in transentorhinal region measured from longitudinal MRI²
- ▶ Previously only observed at autopsy

²Tward, Daniel J., et al. "Entorhinal and transentorhinal atrophy in mild cognitive impairment using longitudinal diffeomorphometry." *Alzheimer's & Dementia: Diagnosis, Assessment & Disease Monitoring* 9 (2017): 41-50.

3. Transformation

Studying transformations quantifies growth or atrophy



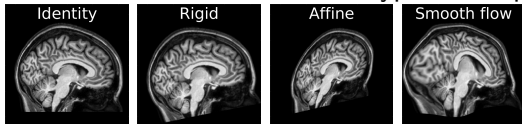
- ▶ Here thickness change in transentorhinal region measured from longitudinal MRI²
- ▶ Previously only observed at autopsy

²Tward, Daniel J., et al. "Entorhinal and transentorhinal atrophy in mild cognitive impairment using longitudinal diffeomorphometry." *Alzheimer's & Dementia: Diagnosis, Assessment & Disease Monitoring* 9 (2017): 41-50.

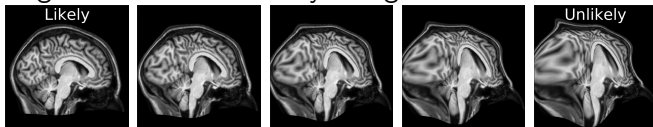
The ingredients of a brain mapping tool

Mappings are calculated from optimization problem with 3 parts.

Transformation model: What types of mappings do we consider?



Regularization: How likely is a given transformation?

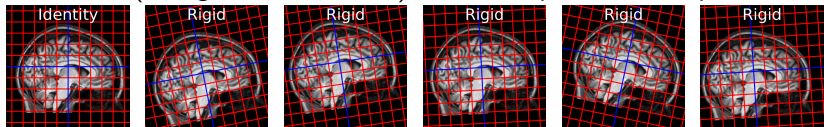


Similarity: How good is an alignment?

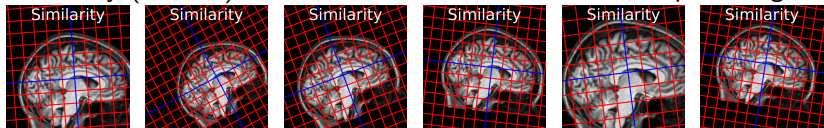


Transformation models: Matrix groups

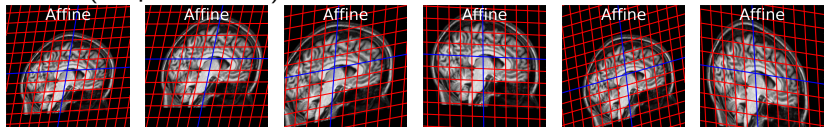
Euclidean (6 degrees of freedom): Encodes position and pose



Similarity (7 DOF): Include scale, more flexible, no shape change



Affine (12 parameters): Include shear and nonuniform scale

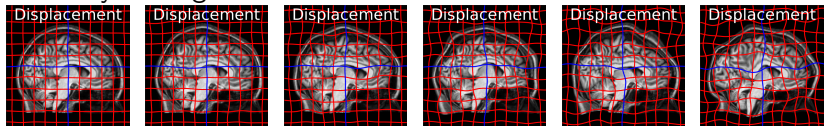


Pros: Simple to compute, easy to enforce invertibility, good for within-subject, often used in conjunction with deformations

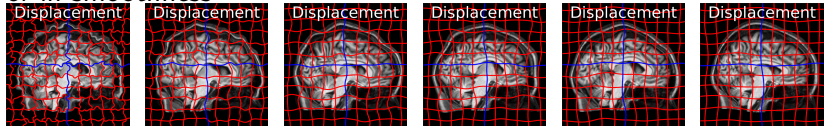
Cons: Cannot model distortions or realistic biological variability

Transformation models: Displacement fields

Can vary in magnitude

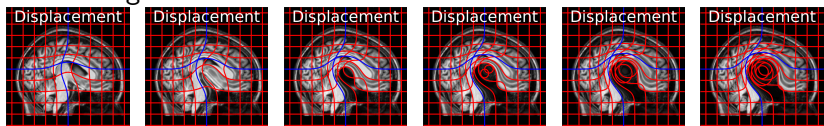


or in smoothness



Pros: Can model a wide range of biological variability.

Cons: Large transforms fail to be invertible no matter how smooth



Transformation models: Flow fields

Composition of invertible transforms is invertible.

We use this to move from displacement to velocity.

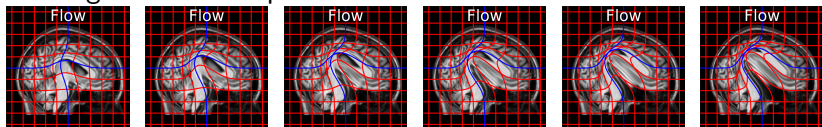
If Δtv_i is a small displacement field, then the composition

$$\varphi_n = (id + \Delta tv_n) \circ \cdots \circ (id + \Delta tv_2) \circ (id + \Delta tv_1)$$

becomes a flow

$$\frac{1}{\Delta t}(\varphi_{n+1} - \varphi_n) = v_n(\varphi_n) \rightarrow \frac{d}{dt}\varphi_t = v_t(\varphi_t)$$

which gives Euler's equation in the limit.



These **diffeomorphisms** form the basis of **Computational Anatomy**, as well as state of the art image registration algorithms.

Pros: Geometric and statistical advantages (discussed below).

Cons: Computational complexity.

Regularization

High dimensional transformations are not unique, regularization allows us to choose **most favorable**.

Early approaches used (e.g.) elastic energy. For φ a transform:

$$\int \frac{1}{2} |D(\varphi - id)(x)|_F^2 dx$$

Computational Anatomy³ uses kinetic energy Lagrangian:

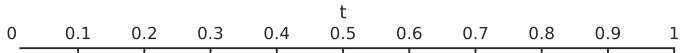
$$\int_0^1 \frac{1}{2} \int |L v_t(x)|^2 dx dt$$

where L is an inertial (differential) operator.

Choosing L with sufficient derivatives **guarantees** diffeomorphisms.

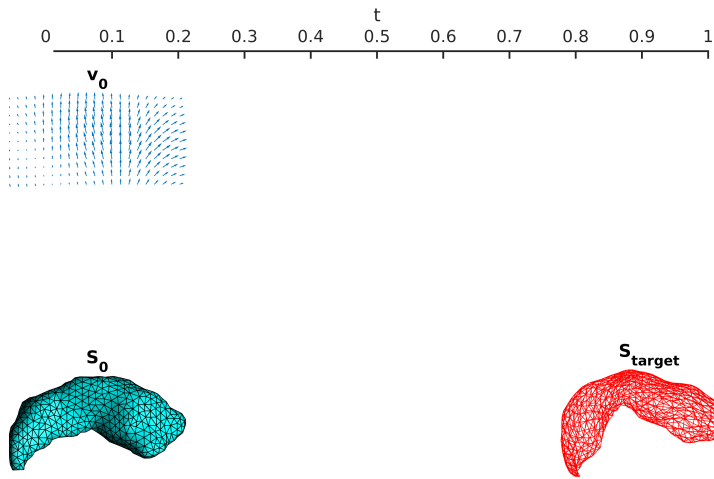
³Beg, M. Faisal, et al. "Computing large deformation metric mappings via geodesic flows of diffeomorphisms." International journal of computer vision 61.2 (2005): 139-157.

Regularization



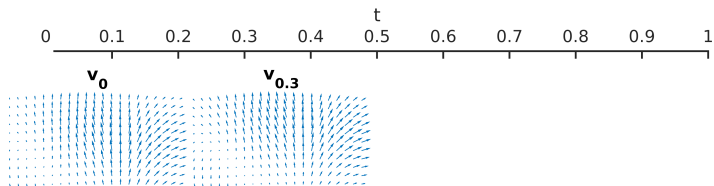
Puts shapes and diffeomorphisms in a Riemannian metric space.
Allows statistical concepts such as averages or regression.

Regularization



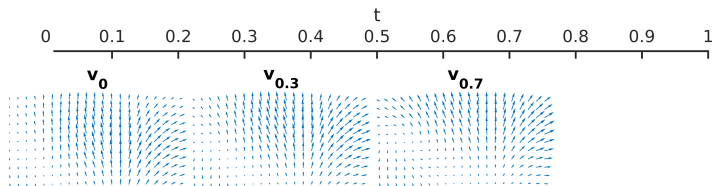
Puts shapes and diffeomorphisms in a Riemannian **metric space**.
Allows statistical concepts such as averages or regression.

Regularization



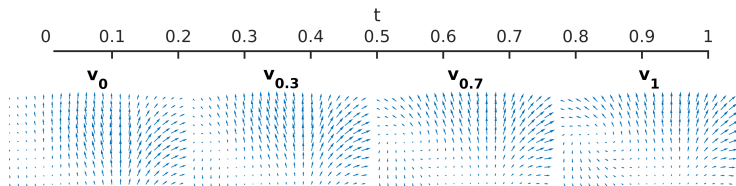
Puts shapes and diffeomorphisms in a Riemannian metric space.
Allows statistical concepts such as averages or regression.

Regularization



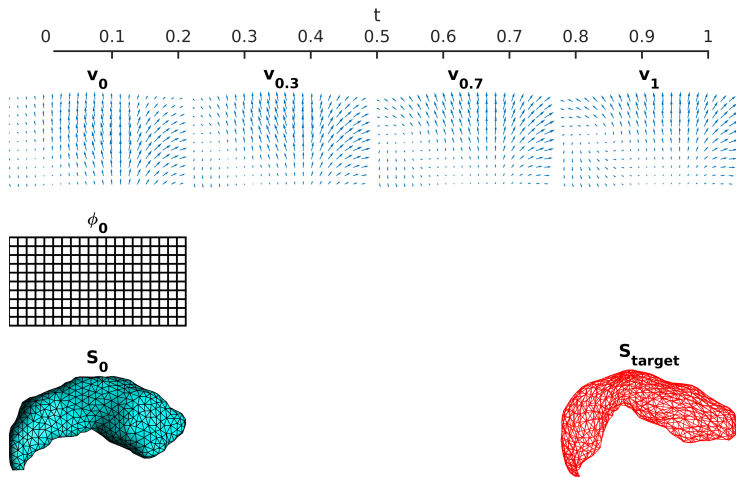
Puts shapes and diffeomorphisms in a Riemannian metric space.
Allows statistical concepts such as averages or regression.

Regularization



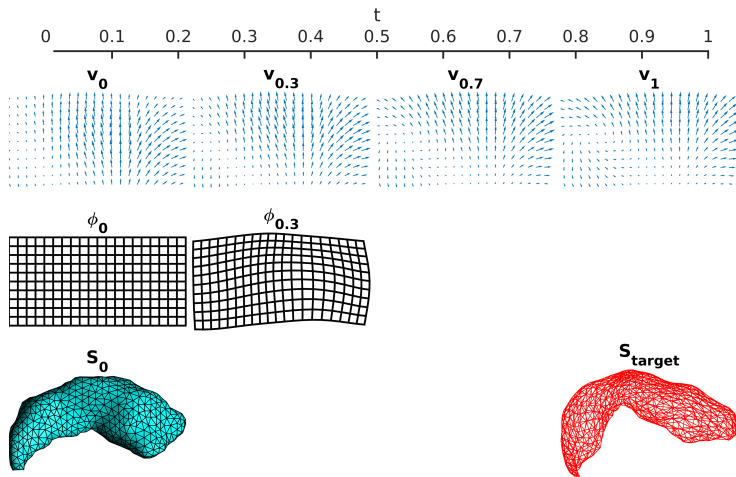
Puts shapes and diffeomorphisms in a Riemannian metric space.
Allows statistical concepts such as averages or regression.

Regularization



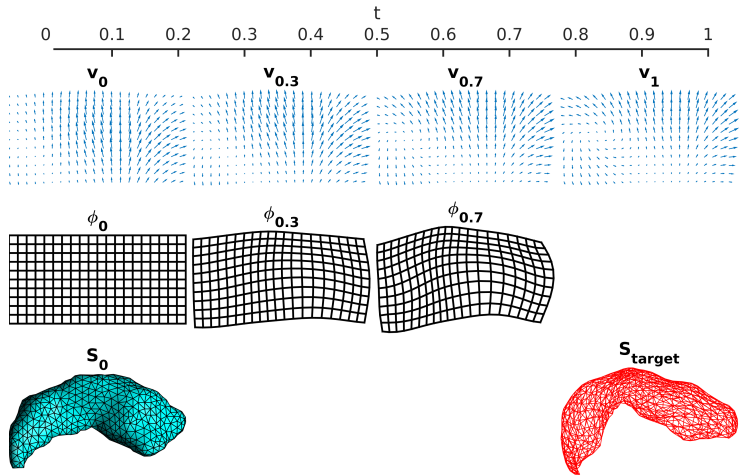
Puts shapes and diffeomorphisms in a Riemannian metric space.
Allows statistical concepts such as averages or regression.

Regularization



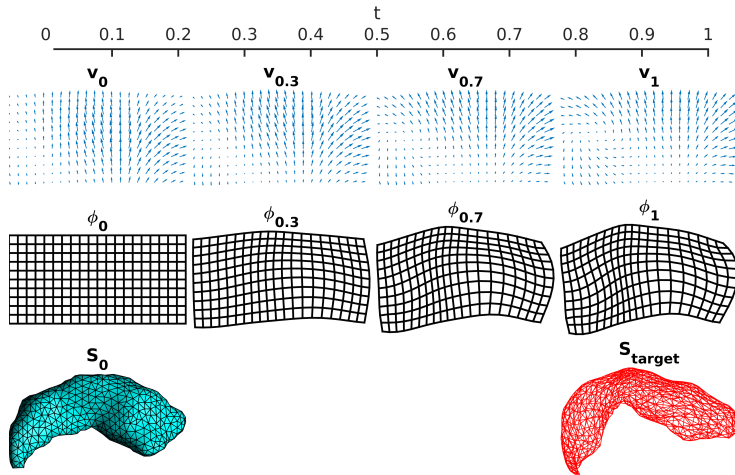
Puts shapes and diffeomorphisms in a Riemannian metric space.
Allows statistical concepts such as averages or regression.

Regularization



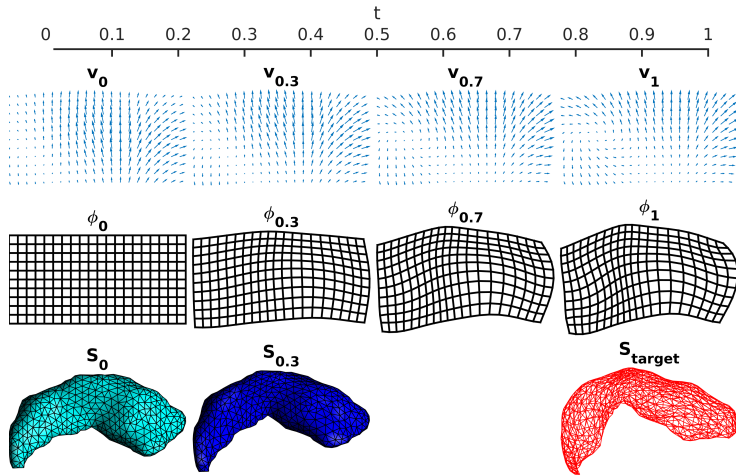
Puts shapes and diffeomorphisms in a Riemannian metric space.
Allows statistical concepts such as averages or regression.

Regularization



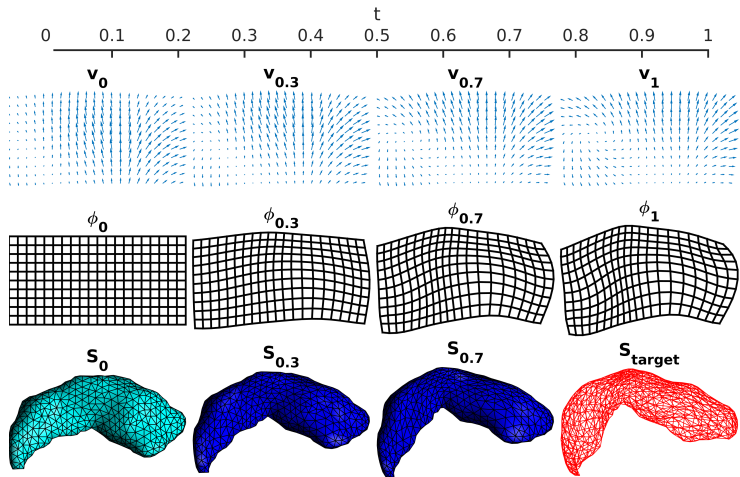
Puts shapes and diffeomorphisms in a Riemannian metric space.
Allows statistical concepts such as averages or regression.

Regularization



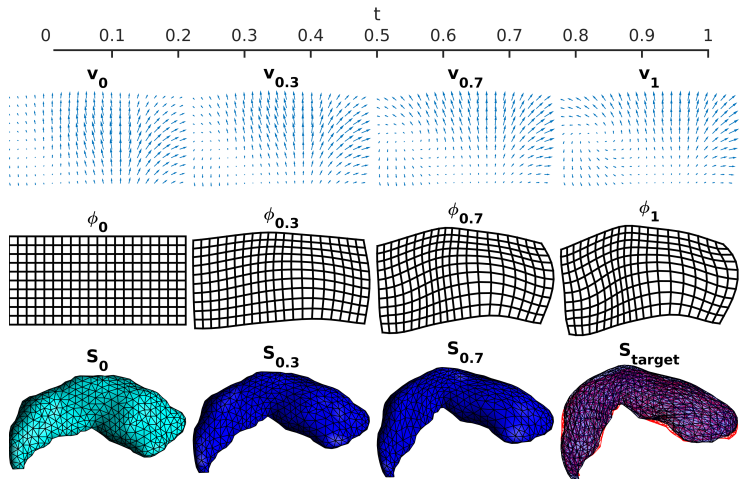
Puts shapes and diffeomorphisms in a Riemannian metric space.
Allows statistical concepts such as averages or regression.

Regularization



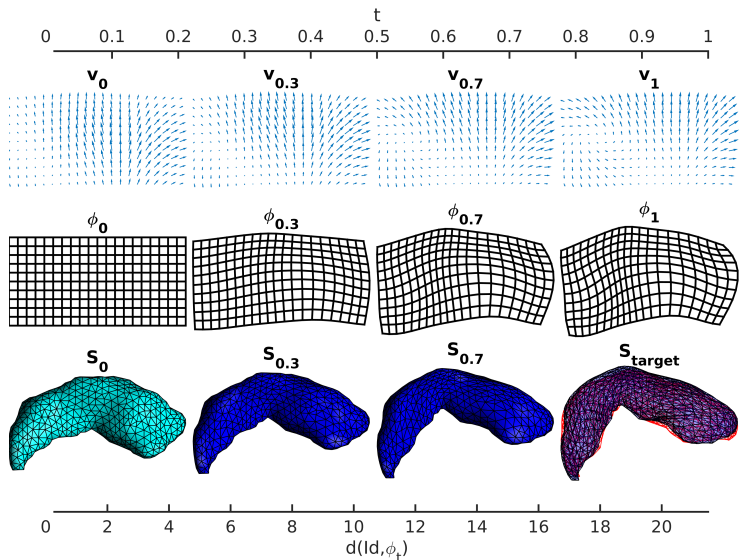
Puts shapes and diffeomorphisms in a Riemannian metric space.
Allows statistical concepts such as averages or regression.

Regularization



Puts shapes and diffeomorphisms in a Riemannian metric space.
Allows statistical concepts such as averages or regression.

Regularization

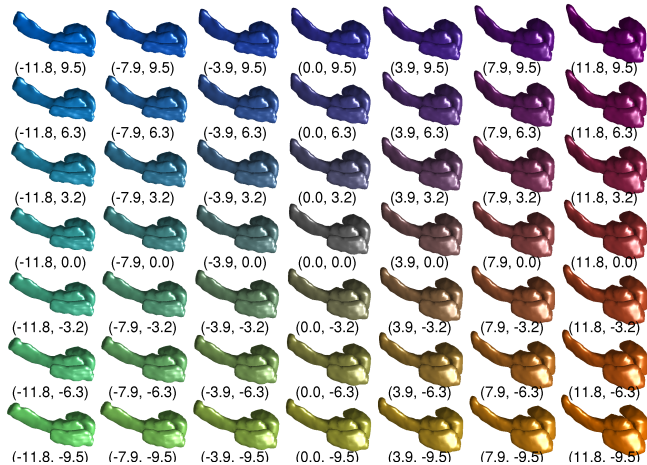


Puts shapes and diffeomorphisms in a Riemannian metric space.
Allows statistical concepts such as averages or regression.

Regularization

Energy minimizing flows admit sparse solutions, key for overcoming bias variance tradeoff in high dimensions

Regularization based on low dimensional priors for MAP estimates⁴



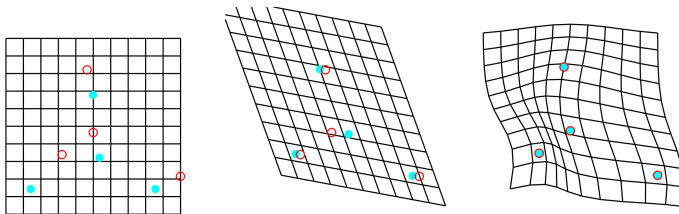
⁴Tward, Daniel, et al. "Parametric surface diffeomorphometry for low dimensional embeddings of dense segmentations and imagery." IEEE transactions on pattern analysis and machine intelligence (2016).

Similarity: Feature point based

Matching corresponding pairs of fiducial landmark points, X to Y , via sum of square error admits closed form solutions:

$$\begin{aligned}\varphi(x) &= Ax \\ A &= \text{Cov}(X, X)^{-1} \text{Cov}(X, Y)\end{aligned}\quad \left.\right\} \quad (\text{affine})$$

$$\begin{aligned}\varphi(x) &= x + \sum_i K(x, X_i) P_i \\ P &= K(X, X)^{-1} (Y - X)\end{aligned}\quad \left.\right\} \quad (\text{spline displacement})$$



Unlabeled points curves and surfaces via currents or varifolds.

Points require manual selection, only ensures accuracy nearby.

Similarity: Image based

Common cost functions for comparing atlas $I(\varphi^{-1})$ to target J :

Voxel based (intra modality), e.g. sum of square error

$$\int \frac{1}{2} |I(\varphi^{-1}(x)) - J(x)|^2 dx$$

conditional likelihood of J given φ in a Gaussian white noise model.
Other robust similarities can be used such as L1 or Huber.

Neighborhood based (inter modality), e.g. MIND⁵ or other local structure, local cross correlation.

Histogram based (inter modality), e.g. mutual information.

⁵Heinrich, Mattias P., et al. "MIND: Modality independent neighbourhood descriptor for multi-modal deformable registration." Medical image analysis 16.7 (2012): 1423-1435.

Challenges and solutions

Most brain mapping techniques were developed for medical imaging, but neuroscience data faces unique challenges:

- ▶ Incomplete or sliced data
- ▶ Artifacts or damaged tissue
- ▶ Multiple different modalities or appearance



We use machine learning to predict one image from another, while **jointly** performing registration and artifact detection⁶



⁶Tward, Daniel Jacob, et al. "Diffeomorphic registration with intensity transformation and missing data: Application to 3D digital pathology of Alzheimer's disease." BioRxiv (2019): 494005.

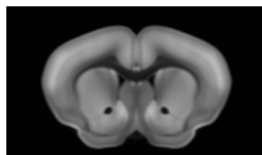
Intensity mapping: Grayscale to grayscale

Expand optimization problem to include an intensity transform F_θ

$$\int \frac{1}{2} |F_\theta[I(\varphi^{-1}(x))] - J(x)|^2 dx$$

and optimize jointly over φ and θ .

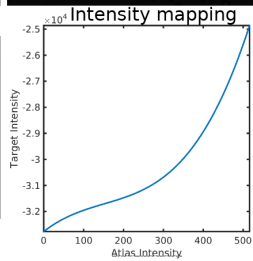
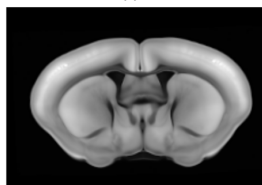
Atlas image I (Allen CCF)



Observed image J (tracing)



Prediction $F_\theta(I)$



Calibration curve: reduce contrast at low intensity, increase at high.

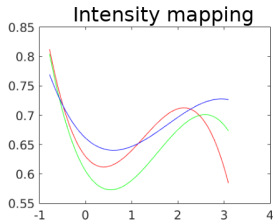
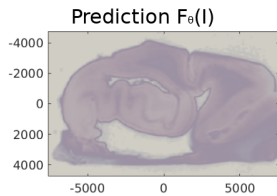
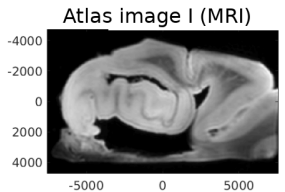
Devin Crowley (devin.g.crowley@gmail.com) Johns Hopkins University Brain mapping tools for neuroscience

Intensity mapping: Grayscale to RGB

Expand optimization problem to include an intensity transform F_θ

$$\int \frac{1}{2} |F_\theta[I(\varphi^{-1}(x))] - J(x)|^2 dx$$

and optimize jointly over φ and θ .



Nonmonotonic: swaps order of “grey”, “white”, “background”.

Devin Crowley (devin.g.crowley@gmail.com) Johns Hopkins University Brain mapping tools for neuroscience

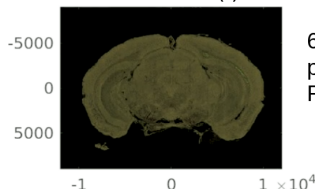
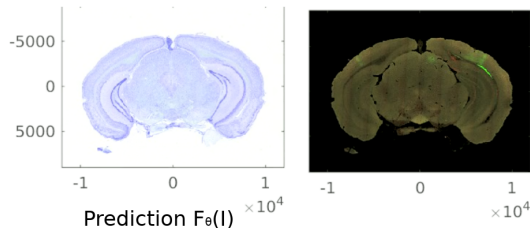
Intensity mapping: RGB to RGB

Expand optimization problem to include an intensity transform F_θ

$$\int \frac{1}{2} |F_\theta[I(\varphi^{-1}(x))] - J(x)|^2 dx$$

and optimize jointly over φ and θ .

Atlas image I (nissl) Observed image J (fluoro)



60 parameter cubic
polynomial map from
 R^3 to R^3

Mix powers of RGB, fairly high dimensional, flexible transforms.

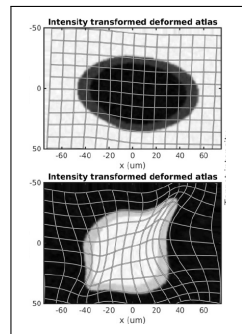
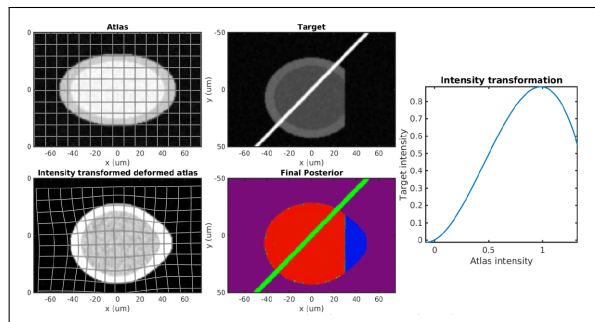
Artifacts

Allows multimodality registration with simple Gaussian likelihood.
Handle artifacts with Expectation Maximization algorithm

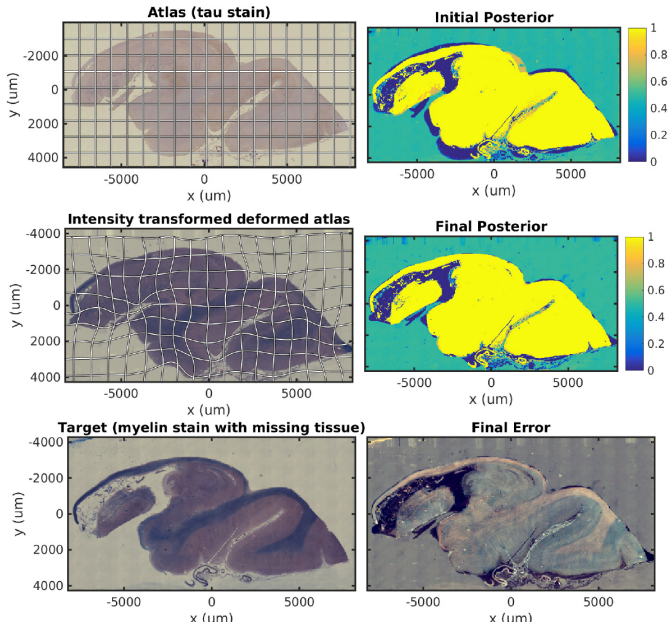
$$\int \frac{1}{2} |F_{\theta}[I(\varphi^{-1}(x))] - J(x)|^2 W(x) dx$$

E step: Compute W as posterior probability for fixed θ, φ .

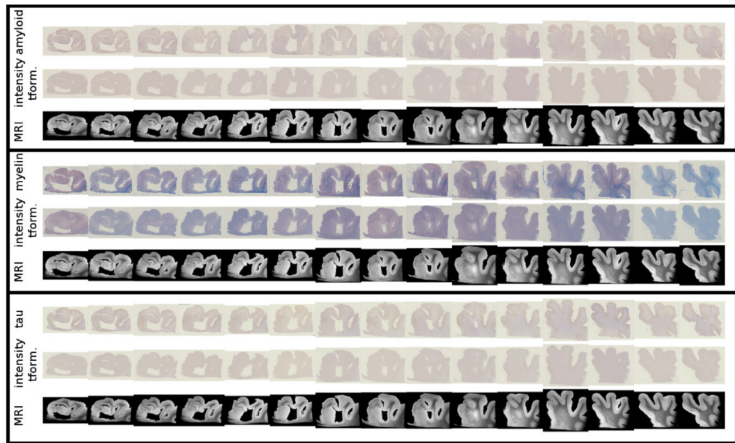
M step: Compute optimal θ, φ for fixed W .



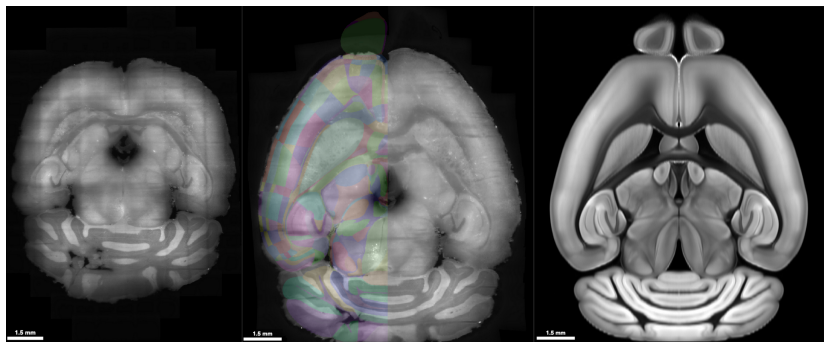
Multimodality and damaged tissue in digital pathology



Multimodal 2D histology slices to 3D atlas



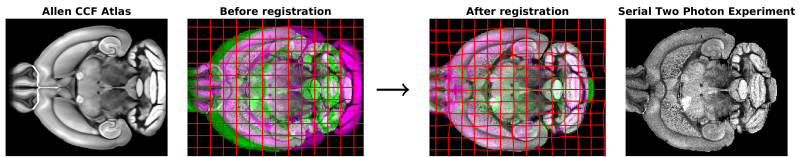
CLARITY cleared mouse brain registered to Allen Atlas



ARDENT⁷: NeuroData's open source brain mapping tool

Publications and code available online from neurodata.io/reg

Ingredient	Choice	Benefit
Transform	Diffeomorphism	Smooth invertible fluid transform
Similarity	Log likelihood	Enables statistical approaches to artifacts and multi-modality
Regularization	Kinetic energy	Enables sparse representations effective in high dimensional bias variance tradeoff ^{5,6}



⁷ Affine and Regularized Diffeomorphic Numeric Transform. ⁸Tward, Daniel, et al. "Parametric surface diffeomorphometry for low dimensional embeddings of dense segmentations and imagery. IEEE transactions on pattern analysis and machine intelligence (2016) ⁹Tward, Daniel, et al. "Estimating diffeomorphic mappings between templates and noisy data: Variance bounds on the estimated canonical volume form. Quarterly of Applied Mathematics (2019).

Computation

Computational burden⁷ includes interpolation:

- ▶ integrating flows
- ▶ deforming images

and Fast Fourier Transforms:

- ▶ applying differential operators
- ▶ inverting differential operators

both are very efficiently parallelized.

We use pytorch (pytorch.org) as interface to GPU computing.

Registration algorithm is about 200 lines of code.

Optimization with gradient descent.

⁷Tward, Daniel J., et al. "Performance of Image Matching in the Computational Anatomy Gateway: CPU and GPU Implementations in OpenCL." Proceedings of the Practice and Experience in Advanced Research Computing 2017 on Sustainability, Success and Impact. ACM, 2017.

Acknowledgements

People

- ▶ Michael Miller (JHU)
- ▶ Joshua Vogelstein (JHU)
- ▶ Susumu Mori (JHU)
- ▶ Juan Troncoso (JHU)
- ▶ Marilyn Albert (JHU)
- ▶ Partha Mitra (CSHL)
- ▶ Brian Lee (JHU)
- ▶ Vikram Chandrashekhar (JHU)
- ▶ Devin Crowley (JHU)

Funding

- NIH: P41EB015909, R01NS086888, R01EB020062, R01NS102670, U19AG033655, R01MH105660, P50AG05146
- NSF: 16-569 NeuroNex contract 1707298, ACI1548562 (Extreme Science and Engineering Discovery Environment)
- Kavli Neuroscience Discovery Institute, BrightFocus Foundation, Dana Foundation